Visualizing the phenomena of wave interference, phase-shifting and polarization by interactive computer simulations

2015 Eur. J. Phys. 36 055016

(http://iopscience.iop.org/0143-0807/36/5/055016)

IOP Publishing European Journal of Physics
Eur. J. Phys. **36** (2015) 055016 (10pp) doi:10.1088/0143-0807/36/5/055016

Visualizing the phenomena of wave interference, phase-shifting and polarization by interactive computer simulations

Uriel Rivera-Ortega and Joris Dirckx

Laboratory of Biomedical Physics, University of Antwerpen, Antwerpen 171, Belgium

E-mail: mecatronica00@hotmail.com

Received 15 April 2015, revised 21 May 2015
Accepted for publication 28 May 2015
Published 15 July 2015

Abstract

In this manuscript a computer based simulation is proposed for teaching concepts of interference of light (under the scheme of a Michelson interferometer), phase-shifting and polarization states. The user can change some parameters of the interfering waves, such as their amplitude and phase difference in order to graphically represent the polarization state of a simulated travelling wave. Regarding to the interference simulation, the user is able to change the wavelength and type of the interfering waves by selecting combinations between planar and Gaussian profiles, as well as the optical path difference by translating or tilting one of the two mirrors in the interferometer setup, all of this via a graphical user interface (GUI) designed in MATLAB. A theoretical introduction and simulation results for each phenomenon will be shown. Due to the simulation characteristics, this GUI can be a very good non-formal learning resource.

S Online supplementary data available from stacks.iop.org/EJP/36/055016/mmedia

Keywords: interferometry, polarization, simulation, phase-shifting

1. Interference and polarization of light

It is possible to represent N optical fields with elliptical polarization and travelling in z direction in form of a vector (omitting by simplicity the temporal and spatial dependencies) as:

$$\mathbf{E}_n = \left(\mathbf{i}E_{nx} + \mathbf{j}E_{ny}\mathrm{e}^{\mathrm{i}\delta_n}\right)\mathrm{e}^{\mathrm{i}\phi_n}, \tag{1}$$

where n goes from $1...N$; E_{nx}, E_{ny}, δ_n are the amplitudes and relative phase difference between each wave component respectively and ϕ_n is associated with the phase of the wave. The state of polarization of a wave is related to its relative amplitudes and phase difference, which describes the shape and orientation of the path traced by the electric field [1]; as a particular example, if $\delta_n = \pm m\pi$ where m is an integer number, the resulting wave will be linearly polarized. An elliptical polarization will result for any other set of amplitudes and relative phases including a circular case when $E_{nx} = E_{ny}$ and $\delta_n = (2m + 1)\pi/2$. Depending on the sign of δ_n, the rotation of the polarization state can be either clockwise or counterclockwise (figure 1).

If light from a source is divided in two beams to be superposed again at any point in space, the intensity in the superposition area varies from maxima (when two waves crests reach the same point simultaneously) to minima (when a wave trough and a crest reach the same point); having as a consequence what is known as an interference pattern or interferogram. Mathematically the resulting interfering wave is the vector addition $\mathbf{E}_T = \sum_{n=1}^{N}\mathbf{E}_n$; if observed by a detector, the result is the average of the field energy per unit area during its integration time that is, the irradiance (I), which can be demonstrated that is proportional to the squared module of the amplitude, however it is usually accepted the approximation $I = \left|\mathbf{E}_T\right|^2 = \left|\sum_{n=1}^{N}\mathbf{E}_n\right|^2$. The fringe visibility (v) resulting from the interference of two beams with linear polarization states is described as $v = \left|\left[2\sqrt{I_1I_2}/(I_1 + I_2)\right]\cos\gamma\right|$, where γ is the angle between the two states of polarization and I_1, I_2 are the irradiances corresponding to each interfering wave [2]. As a particular case for the interference simulation based on a Michelson interferometer presented in this manuscript, it is considered that the irradiance of both beams are comparable and $\gamma = 0$ causing a maximum visibility in the interferogram.

An interferometer is an instrument generally used to generate wave light interference to measure with high accuracy small deformations of the wave front which can be related for instance to surfaces thicknesses, surface roughness, optical power, material homogeneity, distance measurements, etc. In a two wave interferometer one wave is typically flat, known as the reference beam and the other is a distorter wavefront whose shape is to be measured, this beam is known as the probe beam. The general scheme of a two wave interferometer can be observed in figure 2, where the electromagnetic wave $\mathbf{E}$ is typically divided in two coherent parts that is, in a wave $\mathbf{E}_1$ and $\mathbf{E}_2$, where $\mathbf{E}_1$ is the reference wave and $\mathbf{E}_2$ is the probe wave. After the waves have travelled along two separated arms and they have accumulated phase delays, they recombine again by means of a beam splitter giving as a result a field $\mathbf{E}_T$.

The corresponding irradiance due to the interference of two waves can be expressed as

$$I = \left|\mathbf{E}_T\right|^2 = \left|\mathbf{E}_1 + \mathbf{E}_2\right|^2 = \left|\mathbf{E}_1\right|^2 + \left|\mathbf{E}_2\right|^2 + 2\mathrm{Re}\left\{\mathbf{E}_1{}^* \cdot \mathbf{E}_2\right\}, \tag{2}$$

where

$$\left|\mathbf{E}_n\right|^2 = \mathbf{E}_n \cdot \mathbf{E}_n{}^* = \left[\left(\mathbf{i}E_{nx} + \mathbf{j}E_{ny}\mathrm{e}^{\mathrm{i}\delta_n}\right)\mathrm{e}^{\mathrm{i}\phi_n}\right] \cdot \left[\left(\mathbf{i}E_{nx} + \mathbf{j}E_{ny}\mathrm{e}^{-\mathrm{i}\delta_n}\right)\mathrm{e}^{-\mathrm{i}\phi_n}\right] = E_{nx}{}^2 + E_{ny}{}^2, \tag{3}$$

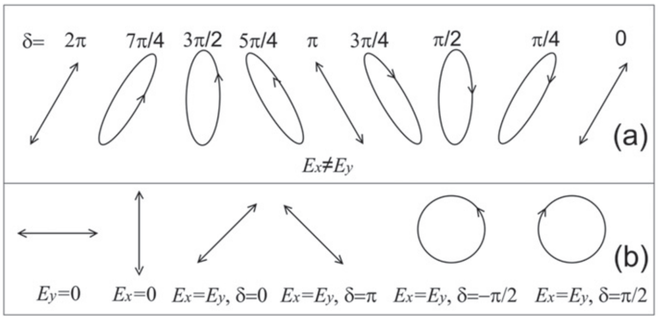

Figure 1. Polarization state figures resulting from different values of phase difference δ and amplitudes E_x, E_y.

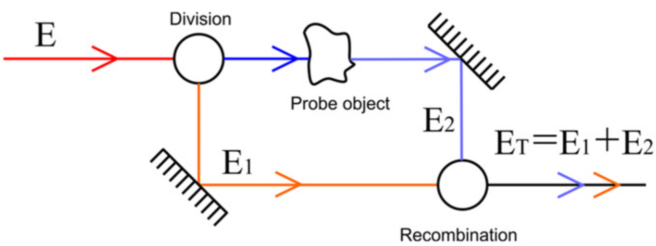

Figure 2. Scheme of a two wave interferometer with a probe object in one beam.

for $n = 1,\ 2$ and

$$\mathbf{E}_1{}^* \cdot \mathbf{E}_2 = \left[\left(\mathbf{i}E_{1x} + \mathbf{j}E_{1y}\mathrm{e}^{-\mathrm{i}\delta_1}\right)\mathrm{e}^{-\mathrm{i}\phi_1}\right] \cdot \left[\left(\mathbf{i}E_{2x} + \mathbf{j}E_{2y}\mathrm{e}^{\mathrm{i}\delta_2}\right)\mathrm{e}^{\mathrm{i}\phi_2}\right]; \tag{4}$$

therefore the resulting interference term is

$$2\mathrm{Re}\left\{\mathbf{E}_1{}^* \cdot \mathbf{E}_2\right\} = 2E_{1x}E_{2x}\ \cos\ \phi + 2E_{1y}E_{2y}\ \cos(\phi + \delta), \tag{5}$$

$\delta = \delta_2 - \delta_1$ and $\phi = \phi_2 - \phi_1$. By taking equations (3)–(5) a general expression for the interference of two waves is obtained

$$I = a_x + b_x\ \cos\ \phi + a_y + b_y\ \cos(\phi + \delta), \tag{6}$$

where $a_x = E_{1x}{}^2 + E_{2x}{}^2$, $a_y = E_{1y}{}^2 + E_{2y}{}^2$, $b_x = 2E_{1x}E_{2x}$ y $b_y = 2E_{1y}E_{2y}$. By applying the identities $A\cos\ \phi + B\sin\ \phi = C\cos(\phi + \psi)$ if $C = \sqrt{A^2 + B^2}$ and $\tan\ \psi = B/A$ to equation (6)

$$I = a + b\ \cos(\phi + \psi), \tag{7}$$

in which a is known as the background light, b as the modulation light and ψ indicates an additional phase shifting, which can be expressed by

$$a = a_x + a_y;\ b^2 = b_x^2 + 2b_xb_y\ \cos\delta + b_y^2;\ \tan\ \psi = \frac{b_y\ \sin\ \delta}{b_x + b_y\ \cos\ \delta}. \tag{8}$$

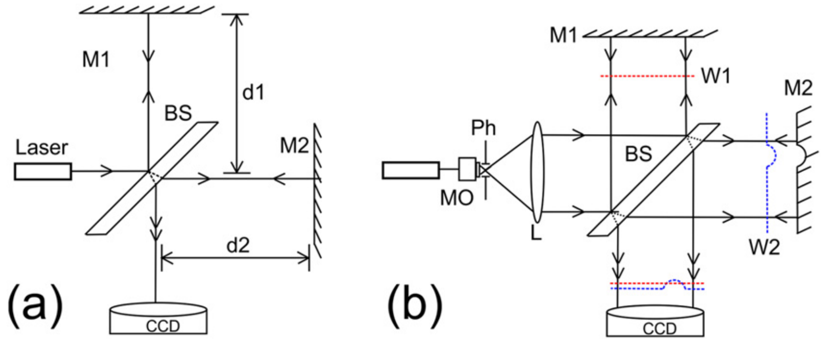

Figure 3. Scheme of (a) Michelson and (b) Twyman–Green interferometer.

2. Phase-shifting interferometry (PSI)

PSI is a technique used to calculate the phase of a probe. In this technique commonly a known reference wave front is moved along its propagation direction respecting to a probe wave front changing with this the phase difference between them (however either of the wavefronts could be moved) [3, 4]. The phase of the resulting wave can be determined by measuring the irradiance changes corresponding to each phase shift. Its mathematical representation can be written as $I_n(x, y) = a(x, y) + b(x, y)\cos\left[\phi(x, y) + \psi_n\right]$, where a is the background illumination, b the fringe modulation, ϕ the object phase, and $\psi_n = 2\pi n/N$ the phase shifting step, which is kept spatially constant at least during the capture time of the interferogram I_n, with $n = 1, \ldots, N$ and N meaning the number of phase steps. For $N \geqslant 3$ a resoluble set of equations is formed because a, b and ϕ are considered temporally constant [5, 6], which implies that the visibility is kept constant when the phase-step is generated, which permits to calculate the phase of the object at each pixel in the image $\phi(x, y)$. As an example, one of the methods used to calculate this phase is the 'four steps technique' [3–5], where the phase is calculated by $\phi = \tan^{-1}\left[(I_4 - I_2)/(I_1 - I_3)\right]$. A more general theory can be proposed when ψ_n is unknown and arbitrary; in this case the method is called generalized phase-shifting interferometry (GPSI) where N equations are obtained but $N + 3$ unknowns are present, and the solution cannot be obtained under the usual PSI theory. However, numerous methods for giving solution at this problem have been successfully introduced.

Experimentally, in PSI and GPSI a phase-step can be introduced using different methods; for instance, by changing the optical path using a mirror on a piezoelectric transducer [7], by inducing changes in the refractive index [8], by means of tilting a glass plate [9], using frequency shifts between the two interfering beams induced by the Zeeman effect [10] or wavelength variations with the Doppler effect [11]. Further techniques include the modulation of polarization [12], a lateral displacements of a grating [13], or a wavelength tunability of a laser diode [14], among others. As a particular case, in this manuscript the phase shifting has been simulated by tilting and/or translating a movable mirror corresponding to one of the arms of a Michelson interferometer.

2.1. Phase-shifting by translating a mirror

This method is based on changing the optical path of a beam by means of moving a mirror that is in the beam trajectory. This movement can be commonly made by using a piezoelectric transducer or a linear translation stage [7]. The phase-shifting is given by $\psi = (2\pi/\lambda)(\text{opd})$, where opd is the optical path difference (OPD). Examples of interferometers with phase-shifting generated by a piezoelectric are: Michelson (figure 3(a)), Twyman–Green (figure 3(b)), Mach–Zehnder which make a phase-shifting by moving a mirror placed in the reference beam trajectory and Fizeau, in which the phase-shifting is made by the translations in either the reference or probe beam.

As a particular case in a Michelson setup (figure 3(a)), if uncollimated light or an extended source is used opd $= 2nd \ \cos \ \theta$, where n is the index of refraction of the medium contained between the mirrors, $d = |d1 - d2|$, where $d1$, $d2$ are the distances of the two mirror from the beamsplitter, therefore because the light beams 1 and 2 travel twice the lengths $d1$ and $d2$, the two beams present a path difference of $2d$ which can be changed by displacing of one of the mirrors (M1, M2). θ is the angle that the incident ray forms with the normal of the mirrors. Figure 3(b) represents an schematic diagram of a Twyman–Green interferometer, in which the light from a laser has been expanded, filtered and collimated (by means of a microscope objective MO, a pinhole Ph and a lens L respectively) thus, $\theta = 0$ and the OPD between the wavefronts W1 and W2 becomes opd $= 2nd$. Therefore, the phase-shifting introducing by a mirror displacement in this interferometer setup will be given by $\psi = (2\pi/\lambda)\text{opd}$.

2.2. Tilting a glass plate

Another method to generate phase-shifting is by means of inserting a glass plate in the light beam [9]. The phase-shift ψ is generated when the plate is tilted an angle ϑ respecting to the optical axis hence $\psi = (t/n)(n \ \cos\vartheta' - \ \cos\vartheta)$, where t is the thickness of the plate, n is the refraction index and $k = 2\pi/\lambda$. The angles ϑ and ϑ' are the angles formed by the normal and the light beams outside and inside the plate respectively. A special requirement is that the plate must be placed in a collimated light beam to avoid aberrations.

3. General description of the simulation software

The presented simulation with teaching purposes is based on a graphical user interface (GUI) created in MATLAB. This GUI is designed to be a friendly and useful visual tool for a better understanding of the phenomenon of interference and polarization of light that can be perfectly applicable in graduate or non-graduate university studies. The GUI can be used by either students or professors, allowing the user to change some parameters such as the interfering wavefronts, their inclination and translation, as well as the wavelength of the light source (for the interference simulation). Regarding to the polarization simulation, the amplitude and phase difference of the two components of a resulting wave can be modify in order to obtain different polarization states.

The GUI main window and its respective suboptions are shown in figures 4(a)–(e). In this window the user can find a description of the simulator as well as its operating instructions. A brief demonstration of this GUI can be seen in Media1.

4. Numerical simulations

4.1. Interference simulator

A numerical verification of the exposed theory is carried out in this section by assuming the fields to be, for simplicity

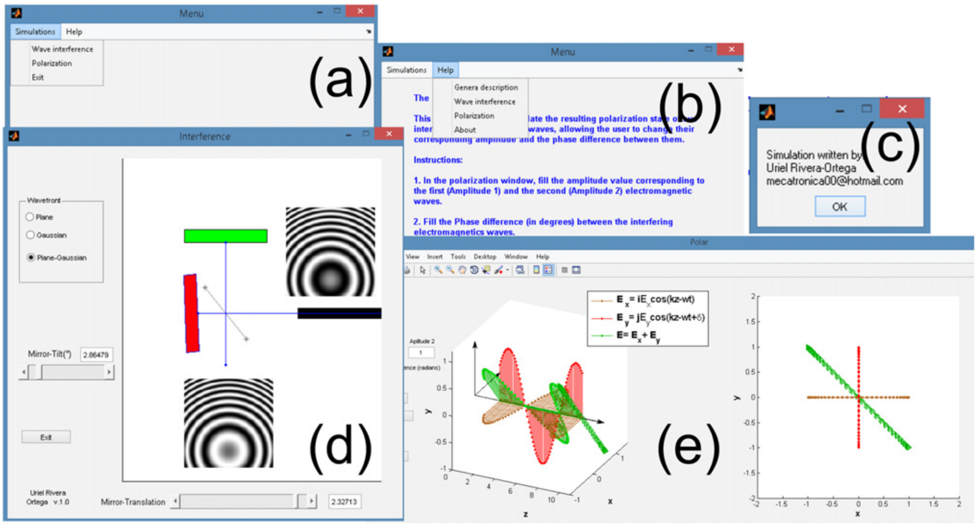

Figure 4. Windows corresponding to each option selected from the main menu (Media1).

$$E_1, E_2 = E = 1,\ \phi_S = x^2 + y^2,\ \phi_P = x\sin\ \theta + y\cos\ \theta, \tag{9}$$

where E_1, E_2 are the amplitudes of each electric field (consequently the interference pattern will have a maximum visibility), ϕ_S, ϕ_P are the phases corresponding to a spherical and planar wave front and θ is the tilt angle of the planar wavefront with respect to the normal of the movable mirror. The electrical fields corresponding to the planar and spherical wavefronts will be treated as monochromatic linearly polarized waves, therefore they can be written as

$$E_p = E\exp\left(\mathrm{i}\phi_P\right),\ E_s = E\exp\left(\mathrm{i}\phi_S\right). \tag{10}$$

The simulated patterns were evaluated on $x \in (-4,\ 4)$ and $y \in (-4,\ 4)$ in a rectangular grid of 150 by 150 points.

Three combinations of two wavefronts can be chosen for the interference simulation, which are: (1) plane–plane, (2) spherical–spherical and (3) plane–spherical (figure 5).

Figure 5 depicts the GUI designed for the interference simulation of the three aforementioned cases. Each of them can be selected by a radio button. The simulation is based on the scheme of a Michelson interferometer setup. The green and red rectangles emulate a fixed and a movable mirror; the laser source and the laser beam are represented with a black rectangle and a blue line respectively, while the dielectric beam splitter is represented with grey line at 45°. In order to emulate the conservation of energy principle, two phase-shifted complementary fringe patterns (due to reflection and phase shifted by π radians) produced by the interference of the selected pair of waves were shown. As an example of the simulation, figures 5(1a)–(c) shows the interference of two plane waves in which the fringes where obtained with the tilt of the movable mirror (red rectangle) and the phase-shift by its displacements, both generated by modifying the value of the knob of two corresponding sliding bars. Figure 5(2) shows the interference of two spherical waves with no inclination. It can be seen that if there is no OPD between the two arms of the interferometer, a field of uniform irradiance shown as an infinitely wide fringe will be presented (figure 5(2a)). Finally figure 5(3a) shows the interference resulting from a non-tilted planar and a spherical

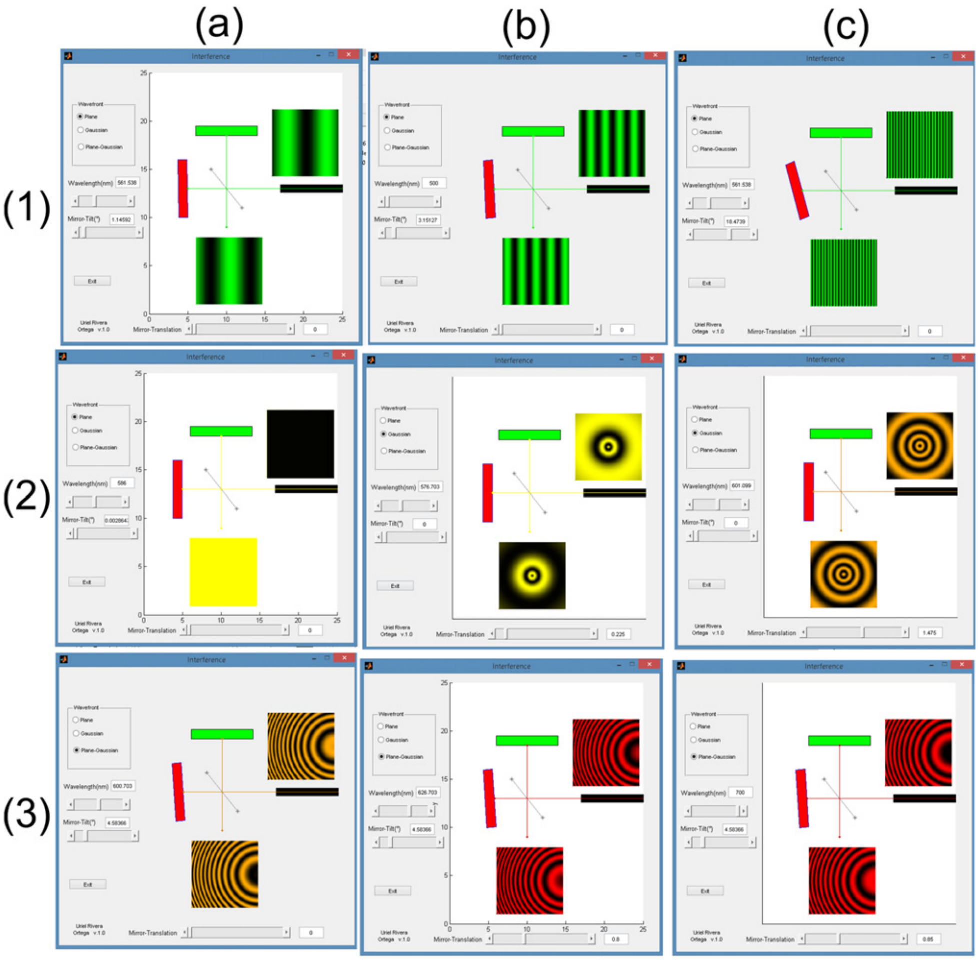

Figure 5. Simulated interference patterns resulting from planar and spherical wavefronts combination with different tilts, displacements of a movable mirror and laser wavelength.

wavefront, and figures 5(3b)–(c) shows the interference pattern resulting from the tilt and translation of the planar wave generated by the movable mirror.

As an additional feature of this simulation, the wavelength of the laser source can be modified also by a sliding bar, which goes from a value of 500 to 700 nm in the visible range. In this way, the user can observe how the output interference patter would be if choosing a different wavelength laser source, also shown in figure 5.

4.2. Polarization simulator

For the polarization simulation consider two orthogonal waves oscillating on x and y-axis and travelling in z-direction

$$\mathbf{E}_x = \mathbf{i}E_x \cos(kz - wt), \tag{11}$$

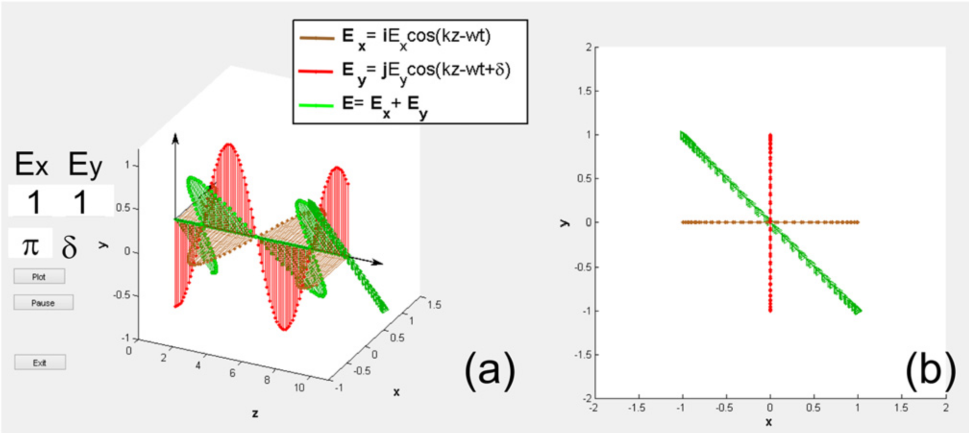

Figure 6. Two orthogonal waves oscillating along the x and y-axis and travelling in z, with their resultant describing a polarization state depicted with a Lissajous figure.

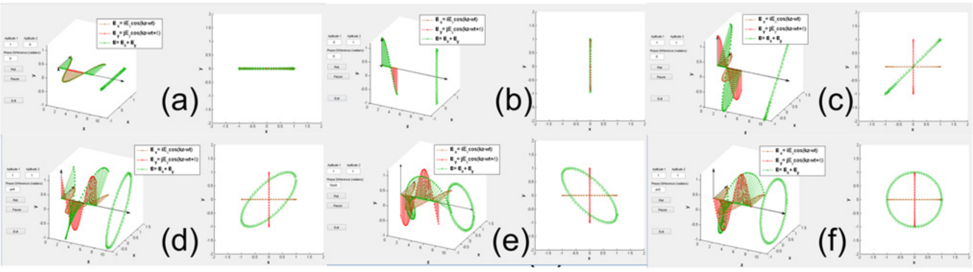

Figure 7. Simulations corresponding to linear (a)–(c), elliptical (d)–(e) and circular polarization states (f).

$$\mathbf{E}_y = \mathbf{j}E_y \ \cos(kz - wt + \delta). \tag{12}$$

E_x, E_y are the scalar amplitudes, **i**, **j** the unitary vectors in x and y directions, w, t the angular frequency and time, with δ as the relative phase between the waves. The resultant optical wave is the vector sum of the two orthogonal waves, described as:

$$\mathbf{E} = \mathbf{E}_x + \mathbf{E}_y. \tag{13}$$

The presented simulation allows the user to see the evolution in time of the resulting wave and its components as well as the polarization state described by the corresponding Lissajous figure, which makes this simulation a very useful illustrative tool for teaching the concept of polarization in an electromagnetic wave [15]. As an example, a linear polarization state resulting from two orthogonal time-travelling waves with unitary amplitudes E_x, $E_y = 1$ (depicted with a brown and red line respectively) with a phase difference $\delta = \pi$ was simulated while the resulting wave is plotted in green, as shown in figure 6(a). The resulting polarization state can be viewed also in this figure, but a frontal perspective and also the two corresponding wave components are shown in figure 6(b) for a better appreciation.

The input parameters of the polarization simulation given by the user are: the amplitudes E_x, E_y and their phase difference δ. Once given those parameters, the simulation can be started by clicking on the 'plot' button and pause it at any instant by clicking on the 'pause' button. The simulation can be restarted by clicking anywhere inside the simulation window.

In order to show the behaviour of the presented polarization simulation, other polarization states are also depicted. Figures 7(a) and (b) shows linear polarization states, oscillating in the x-axis ($E_x = 1, E_y = 0, \delta = 0$) and y-axis ($E_x = 0, E_y = 1, \delta = 0$) and figure 7(c) show a linear polarization at $\pi/4(E_x = 1, E_y = 0, \delta = 0)$. Two elliptical ($E_x = 1, E_y = 1, \delta = \pi/4$), ($E_x = 1, E_y = 1, \delta = 3\pi/4$) and a circular polarization ($E_x = 1, E_y = 1, \delta = \pi/2$) states are also simulated (figures 7(d)–(f)).

It is worth mentioning that the rotation of the field (clockwise or counterclockwise) due to the phase difference between the components can also be seen by looking at the evolution of the resulting Lissajous figure, which adds an important feature to the present simulation for teaching purposes.

5. General conclusions and remarks

In this manuscript, a GUI designed in MATLAB for the simulation of the phenomena of interference, phase-shifting and polarization of light for didactic purposes has been presented. In some graduate or undergraduate university courses, they are totally explained based on the course book lectures without extra resources, which make the understanding of the topic in some cases a difficult and tedious task. Therefore, this GUI is proposed as a helpful easy to use tool for teachers and students as an informal learning resource [16] by emulating the interference of two waves in an interferometric setup and by observing the time evolution of a polarized wave, allowing the user to change some important parameters such as the OPD and the wavelength of the light source regarding to the interference simulation; and the phase difference and amplitude of the components of a travelling wave concerning to the polarization simulation.

The interference option presents a simulation based on a Michelson interferometer to generate the interference of a plane–plane, plane–spherical and spherical–spherical waves (those wavefronts have been chosen as they are the most commonly used in theory, but they can be easily changed in the algorithm if necessary) by choosing them with a radio button. This interferometer contains a fixed and a movable mirror, which can be tilted and translated by means of moving the knob position of a sliding bar in order to change the number of the interference fringes or to generate a phase-shift by changing the OPD between the mirrors, which also makes this simulation a helpful tool for explaining the concept of PSI or GPSI. The two complementary interference patterns (phase-shifted by π) located in a real Michelson interferometer setup are also simulated in order to show the principle of conservation of energy.

By giving the amplitude values E_x, E_y and the phase difference δ of two orthogonal waves, the polarization simulation shows their evolution in time as well as their resultant wave describing a polarization state forming a Lissajous figure, which makes this simulation a very useful illustrative tool for teaching and visualizing the concept of a travelling electromagnetic wave and polarization. In addition this simulation can be paused so the evolution of the waves and its resultant polarization can be analysed in an instant of time, also allowing to observe the direction of the polarization rotation. These simulations were shown with some example figures and Media 1.

There are many simulations available online in Java platform, which simulates the interference of two waves; however they do not show neither the resulting interference pattern of the two used wavefronts in laboratory demonstrations nor all the adjustable features in one standalone application. Regarding to the polarization, there are some online applet simulators that also show the resulting polarization state by modifying the amplitude and phase difference of a wave components, however some of them do not show the time evolution of the wave (which can also be paused if needed) with an isometric and frontal view which allows a better visual understanding of the phenomena. Finally, in most cases, these simulations cannot be downloaded and they are found separately.

The executable windows standalone application and all the required files needed to run the presented interactive MATLAB GUI simulator can be freely downloaded in the following link: https://drive.google.com/open?id=0Bz9Jz7_ucF7gdWUxVHB1UHViTEk&authuser=0. In the case that the MATLAB Compiler Runtime is needed, the full package can be downloaded from: https://drive.google.com/open?id=0Bz9Jz7_ucF7ga0lNaWRkMVFFaVk&authuser=0.

Acknowledgments

Uriel Rivera-Ortega appreciates the postdoctoral scholarship from Consejo Nacional de Ciencia y Tecnología (México) under grant 230729.

References

[1] Hecht E 2007 *Optics* (San Francisco: Addison-Wesley) pp 326–9
[2] Goodwin E P and Wyant J C 2006 *Field Guide to Interferometric Optical Testing* vol FG10 ed J E Greivenkamp (Washington: SPIE Press) p 6
[3] Schwider J 1990 Advanced evaluation techniques in interferometry *Progress in Optics XXVIII* vol 28 ed E Wolf (Amsterdam: Elsevier) pp 274–6
[4] Malacara D 2007 *Optical Shop Testing* (New York: Wiley) pp 547–50
[5] Creath K 1988 Phase-measurement interferometry techniques *Progress in Optics XXVI* vol 26 ed E Wolf (Amsterdam: Elsevier) pp 358–66
[6] Malacara D, Servin M and Malacara Z 1998 *Interferogram Analysis for Optical Testing* (New York: Dekker) pp 169–245
[7] Ai C and Wyant J C 1987 Effect of piezoelectric transducer nonlinearity on phase shift interferometry *Appl. Opt.* **26** 1112–6
[8] Chen L R 2001 Phase-shifted long-period gratings by refractive index-shifting *Opt. Commun.* **200** 187–91
[9] Xie X, Yang L, Xu N and Chen X 2013 Michelson interferometer based spatial phase shift shearography *Appl. Opt.* **52** 4063–71
[10] Gasvik Kjell J 2002 *Optical Metrology* (England: Wiley) pp 54–6
[11] Malacara D, Rizo I and Morales A 1969 Interferometry and the Doppler effects *Appl. Opt.* **8** 1746–7
[12] Kothiyal P M and Delisle C 1985 Shearing interferometer for phase shifting interferometry with polarization phase shifter *Appl. Opt.* **24** 4439–42
[13] Susuki T and Hioki R 1967 Translation of light frequency by a moving grating *J. Opt. Soc. Am.* **57** 1551
[14] Rivera-Ortega U and Dirckx J 2015 On–off laser diode control for phase retrieval in phase-shifting interferometry *Appl. Opt.* **54** 3576–9
[15] Collett E 2005 *Field Guide to Polarization* vol FG05 ed J E Greivenkamp (Washington: SPIE Press) pp 7–11
[16] Goodwin K, Kennedy G and Vetere F 2010 Getting together out-of-class: using technologies for informal interaction and learning *Proc. Ascilite (Sydney)* pp 387–92